



Muñoz-Salinas, E., Castillo, M., Sanderson, D. C.W. and Cresswell, A. (2018)  
First luminescence geochronology of the beach-dune ridges of Nayarit strand-plain  
(west-central Mexico). *Journal of South American Earth Sciences*, 88, pp. 642-648.  
(doi:[10.1016/j.jsames.2018.08.003](https://doi.org/10.1016/j.jsames.2018.08.003))

There may be differences between this version and the published version. You are  
advised to consult the publisher's version if you wish to cite from it.

<http://eprints.gla.ac.uk/167153/>

Deposited on: 20 August 2018

Enlighten – Research publications by members of the University of Glasgow  
<http://eprints.gla.ac.uk>

# Accepted Manuscript

First luminescence geochronology of the beach-dune ridges of Nayarit strand-plain  
(west-central Mexico)

E. Muñoz-Salinas, M. Castillo, D. Sanderson, A. Creswell



PII: S0895-9811(18)30200-1

DOI: [10.1016/j.jsames.2018.08.003](https://doi.org/10.1016/j.jsames.2018.08.003)

Reference: SAMES 1975

To appear in: *Journal of South American Earth Sciences*

Received Date: 9 May 2018

Revised Date: 5 August 2018

Accepted Date: 5 August 2018

Please cite this article as: Muñoz-Salinas, E., Castillo, M., Sanderson, D., Creswell, A., First luminescence geochronology of the beach-dune ridges of Nayarit strand-plain (west-central Mexico), *Journal of South American Earth Sciences* (2018), doi: 10.1016/j.jsames.2018.08.003.

This is a PDF file of an unedited manuscript that has been accepted for publication. As a service to our customers we are providing this early version of the manuscript. The manuscript will undergo copyediting, typesetting, and review of the resulting proof before it is published in its final form. Please note that during the production process errors may be discovered which could affect the content, and all legal disclaimers that apply to the journal pertain.

## First luminescence geochronology of the beach-dune ridges of Nayarit strand-plain (west-central Mexico)

E. Muñoz-Salinas<sup>1,2,\*</sup>, M. Castillo, D<sup>1,2</sup>, Sanderson<sup>3</sup>, A. Creswell<sup>3</sup>

<sup>1</sup>*Instituto de Geología, Universidad Nacional Autónoma de México, Ciudad Universitaria, Mexico City, Mexico*

<sup>2</sup>*Laboratorio Nacional de Geoquímica y Mineralogía, Ciudad de México, Mexico*

<sup>3</sup>*Scottish Universities Environmental Research Centre, East Kilbride, Glasgow, United Kingdom*

\*e-mail: [Esperanzam@ownmail.net](mailto:Esperanzam@ownmail.net)

### Abstract

Strand-plains are composed by beach-dune ridges that constitute coastal sedimentological records of continental erosion and associated climatic and geological controls on their formation. The strand-plain of Nayarit is one the most prominent strand-plains around the world as it is composed by > 250 well-preserved beach-dune ridges that distributes along > 200 km between the states of Nayarit and Sinaloa (west-central Mexico) and extends for ~14 km inland. Although the strand-plain of Nayarit is of broad interest for understanding the evolution of Quaternary landscapes, it has remained understudied. To contribute to a better understanding of the landscape evolution of the strand-plain of Nayarit we present here a complete geochronology based on sixteen OSL dating ages distributed across three different transects of beach-dune ridges located from the coast towards the inland. Our data indicate that in all cases the oldest ridges initiated ~2 ka. The depositional rates range from ~6 m a<sup>-1</sup> toward the south of the strand-plain, where is located the mouth of Santiago and San Pedro rivers, which are the largest of the study area, to ~1.8 m a<sup>-1</sup> toward the north. These depositional rates are among the highest denudation rates reported in strand-plains around the world. We estimate that the formation of the coastal plain of Nayarit initiated ~6 to 7 ka, which correspond to last period of the global marine stabilization after sea level rise.

**Keywords:** strand-plain, beach-dune ridges, luminescence dating, Nayarit, west-central Mexico

### 1. Introduction

Strand-plains are composed by beach-dune ridges generated by interaction of coastal and aeolian processes along shoreline and formed when there is enough terrigenous sediment in the foreshore, which is usually delivered by rivers (Tamura, 2012). The beach-dune ridges advance seaward producing a sequence of parallel ridges where the youngest are adjacent to the beach and the oldest are located far inland. Because each beach-dune ridge forms in decadal time-scale and it is composed by the sediment resulting from the denudation of the continent, each ridge contains information about the continental erosion, the geologic composition of the continent and the climatic control on the landscape (Nordstrom et al., 1991; Otvos, 2000). Since most of beach-dune ridges have been eroded or buried during the sea-level rise, most of the strand-plains today

contain ridges formed after the last global marine stabilization. Therefore, strand-plains constitute natural records to constrain climatic and geological changes affecting sediment delivering rates to coastal plains after the last ~7 ka (Davis, 2011).

The strand-plain of Nayarit is one of the most prominent strand-plains of the world (Tamura, 2012) which is the result of the vast sediment supplied from many rivers such as the Santiago River that is one of the largest rivers of Mexico (Hudson et al., 2005). The strand-plain contains more than 250 well-preserved beach-dune ridges distributed along > 200 km, between the Mexican states of Nayarit and Sinaloa (west-central Mexico). These beach-dune ridges extend for ~13 km from the coast to inland. Although the strand-plain of Nayarit is of broad interest for understanding the evolution of Quaternary landscapes, due to its well-preserved beach-dune ridges which contain detail information about the sedimentation along the coastal plain and denudation of the continent, this has remained poorly documented. Moreover, the sediment forming these beach-dune ridges contains information of Quaternary landscape dynamic changes of west-central Mexico.

So far the only studies dealing with the landscape evolution of the strand-plain of Nayarit were those published by Joseph Curray and David Moore in the 1970's and the Master of Science thesis of Ruben Abe Cisneros in 2011. Curray and Moore studied the strand-plain of Nayarit inside a research project aimed at the study of the oceanic platform of the California Gulf requested by the Scripps Research Institute, USA (Curray and Moore, 1964; Curray et al., 1969; Moore and Curray, 1969). The authors scanned the ocean floor with high resolution topographic instrumentation and identified the Pleistocene submerged delta of Nayarit. They focused on the Holocene delta that they examined using air photographs and constrained its geochronology by using radiocarbon dating. Abe Cisneros (2011) investigated the source of the sediments composing the beach-dune ridges of the strand-plain of Nayarit Delta using geochemical analysis from a set of samples extracted around the strand-plain and comparing them with the geochemical firm of the main rivers flowing into the strand-plain, which are: Acaponeta, San Pedro and Santiago. As long as the Santiago River transports sediment from the Trans-Mexican Volcanic Belt (TMVB), characterized by basalts and andesites, the geochemical firm was completely different to the one coming from the Acaponeta and San Pedro rivers which transport sediments from the Sierra Madre Occidental (SMO), characterized by rhyolites and ignimbrites. Therefore Abe Cisneros concluded that the Santiago River provides most of the sediment to the foreshore that is returned to the beach to form the beach-dune ridges of the strand-plain of Nayarit (Fig. 1).

The goal of this study is to provide the first luminescence geochronology of the strand-plain of Nayarit and assess the evolution of such landscape. For this purpose, we estimated the ages of 16 samples using the optically stimulated luminescence (OSL) dating technique. Our sampling sites were distributed across three different transects that cross the beach-dune ridges and separated each transect for ~30 to 45 km from north to south along the strand-plain. By this way we obtained a complete record of the oldest and youngest ages of the beach-dune ridges allowing the estimation of their depositional rates.

## 2. Study Area

The strand-plain of Nayarit extends from the coast to inland for ~14 km and distributes along > 200 km from north to south between the towns of San Blas (state of Nayarit) and Mazatlan (state of Sinaloa) (Fig. 1). This landscape is composed by more than 250 beach-dune ridges oriented from N-S and from NNW-SSE. Their crests raise up to 1 m asl and separate for few tens of meters among them. The parallel ridges to the actual shoreline correspond to the youngest period of formation and the oblique ridges are indicative of past changes in the former morphology of the coastal line (Abe Cisneros, 2011; see in Fig. 2 main directions of beach dune ridges). Currently, subparallel ridges are being eroded in some sections of the strand-plain (Cruz González, 2012). Abe Cisneros (2011) identified five periods of shoreface successions based on the geomorphological interpretations of Curray et al. (1969). They propose that the beach-dune ridges initiated 4.7 - 4.5 ka, which is based on radiocarbon dating (see Fig. 2 for the different periods proposed by Abe Cisneros of the strand-plain of Nayarit at the it central sector).

Seven rivers flow into the strand-plain of Nayarit; the four most important based on their drainage area are from north to south: Las Cañas, Acaponeta, San Pedro and Santiago. The Santiago River is one of the largest rivers of Mexico; which sources close to Mexico City at about 3,500 m asl and incises into the western sector of the TMVB, a geological province that contains active stratovolcanoes and monogenetic volcanic fields (Muñoz-Salinas and Castillo, 2013). The rest of the rivers incise into the southern part of the SMO that is constituted mostly by ignimbrites (Fig. 2).

Since 2010 the beach-dune ridges of the strand-plain of Nayarit are protected by Mexican authorities where it was recognized the landscape as Biosphere Reserve known as Marismas Nacionales of Nayarit (<http://www.conanp.gob.mx/>). This landscape is not only of geological value, it also contains endemic and endangered fauna and flora. As a consequence, human activities are restricted, however, this only occurs at about the central part of the strand-plain (across the Santa Cruz transect of Fig. 2) where the landscape contains well-conserved mangrooves and beach-dune ridges. Other parts of the strand-plain are extensively used for agricultural proposes. The characteristic vegetation of the strand-plain is the mangrove, especially the *Rhizophora mangle* what is favored by saline soils and the prevailing climate which is tropical savanna with annual precipitation above 1500 mm.

### 3. Methodology

#### 3.1. Luminescence dating

OSL is based on the study of the luminescence signals emitted by mineral grains when they are stimulated optically in the laboratory (Huntley et al., 1985; Aitken, 1998). This dating method considers that the geochronological clock sets to zero when mineral grains (quartz and feldspars) are exposed to sunlight during transport and prior to deposition and burial. Aeolian mechanisms are the most appropriate to expose grains to sunlight (Duller, 2008; Brill et al., 2015). Aeolian processes play an important role in the formation of beach-dune ridges, because the sediment transported by rivers to the ocean is returned to the shoreline due to wave-dominated sea conditions. The sediment returned to the beach, which is basically composed by sand, generates a berm (i.e. a bar parallel to the coastal line) that will eventually be far from the sea waving

influence, thus, wind will be the main mechanism of re-deposition of grains along the beach. Therefore, beach-dune ridges are adequate landforms to use luminescence dating since sand grains are set to zero prior to their burial (Nielsen et al., 2006; Reimann et al., 2011). The strand-plain of Nayarit contains important proportions of quartz which is used in the OSL analysis. The luminescence dating has proved to be a very accurate method to constrain the geochronological evolution of strand-plain and it has advantages over radiocarbon dating. Mainly, because for radiocarbon dating enough organic matter, produced at the time of beach-dune formation, is required to provide accurate dating results, this condition is sometimes hard to fulfill (Isla and Bujalesky, 2000; Tamura et al., 2017).

### **3.2. Field work**

In February 2017 we carried out the fieldwork to extract a total of 16 samples for OSL dating. The sampling sites were distributed from W-E along three different transects positioned almost perpendicularly and obliquely crossing the beach-dune ridges from the coastal area to inland (see the location of transects in Fig. 2). Samples extracted from transects are located at: 1) Santa Cruz, it is approximately 14 km long with 8 samples extracted, 2) Novillero, it is approximately 45 km to the north of Santa Cruz Transect, is approximately 7 km long with 3 samples extracted; and 3) Toro Mocho, approximately 30 km to the south of Santa Cruz Transect, is approximately 8 km long with 5 samples extracted. We found that beach-dune ridges at Santa Cruz Transect were well-preserved (see Figs. 3A and B) as the mangrove swamp is non-altered by human activities. In the case of Novillero and Toro Mocho transects, we observed cultivated surfaces and as a result, the surface of beach-dune ridges was slightly modified (see Figs. 3C and D). In the case of Santa Cruz Transect, we excavated holes of ~30 to 50 cm to extract samples but in the case of Novillero and Toro Mocho, we excavated holes of a minimum of 80 cm of depth to collect the unaltered sediment due to plowing works.

To obtain the samples for OSL analysis, in the deepest parts of each trench, we introduced a polyethylene tube of 10 cm diameter and 25 cm long inside the sediment of the ridge. We extracted at least 500 g of sediment inside each tube after covering the trench with a dark and opaque blank. When the sediment was extracted in the tube, we wrapped it with aluminum foil in order to keep the sample protected against bleaching. These samples were used for luminescence analysis in the laboratory. On each site, we also extracted about 200 g of the sediment surrounding the tube for dose rate determinations. The coordinates of each site were recorded with a differential GPS (Trimble® Geo7x).

### **3.3. Laboratory**

All OSL samples were analyzed at the Scottish Environmental Research Centre (SUERC) in the United Kingdom using the single aliquot regenerative (SAR) method in grains of quartz (Wintle and Murray, 2006). For further details on the analytical procedures consult the laboratory report of Cresswell et al., (2017).

#### **3.3.1. Dose rate determinations**

Dose rates were performed on the ~500 g of sediment samples extracted in field work using high resolution gamma spectrometry (HRGS) and thick source beta counting (TSBC). HRGS measurements were performed using a 50% relative efficiency “n” type hyper-pure Ge detector (EG&G Ortec Gamma-X) operated in a low background lead shield with a copper liner. Gamma ray spectra were recorded over the 30 keV to 3 MeV range from each sample, interleaved with background measurements and measurements from SUERC Shap Granite standard in the same geometries. Sample counts were for 80 ks. The spectra were analyzed to determine count rates from the major line emissions from  $^{40}\text{K}$  (1461 keV), and from selected nuclides in the U decay series ( $^{234}\text{Th}$ ,  $^{226}\text{Ra}$  +  $^{235}\text{U}$ ,  $^{214}\text{Pb}$ ,  $^{214}\text{Bi}$  and  $^{210}\text{Pb}$ ) and the Th decay series ( $^{228}\text{Ac}$ ,  $^{212}\text{Pb}$ ,  $^{208}\text{Tl}$ ) and their statistical counting uncertainties. Net rates and activity concentrations for each of these nuclides were determined relative to Shap Granite by weighted combination of the individual lines for each nuclide. The internal consistency of nuclide specific estimates for U and Th decay series nuclides was assessed relative to measurement precision, and weighted combinations used to estimate mean activity concentrations ( $\text{Bq kg}^{-1}$ ) and elemental concentrations (% K and ppm U, Th) for the parent activity. These data were used to determine infinite matrix dose rates for alpha, beta and gamma radiation.

Beta doses were also measured directly using the SUERC TSBC system (Sanderson, 1988). Count rates were determined with six replicates 600 s counts on each sample, bracketed by background measurements and sensitivity determinations using the Shap Granite secondary reference material. Infinite-matrix dose rates were calculated by scaling the net count rates of samples and reference material to the working beta dose rate of the Shap Granite ( $6.25 \pm 0.03 \text{ mGy a}^{-1}$ ). The estimated errors combine counting statistics, observed variance and the uncertainty on the reference value.

The dose rate measurements were used in combination with the assumed burial water contents, to determine the overall effective dose rates for age estimation. Cosmic dose rates were evaluated by combining latitude and altitude specific dose rates ( $0.17 \pm 0.01 \text{ mGy a}^{-1}$ ) for the site with corrections for estimated depth of overburden using the method of Prescott and Hutton (1994).

### 3.3.2. Quartz SAR luminescence measurements

All the samples extracted in the polyethylene tubes were prepared and measured in a Risø DA-15 automatic reader equipped with a  $^{90}\text{Sr}/^{90}\text{Y}$   $\beta$ -source for irradiation, blue LEDs emitting around 470 nm and infrared (laser) diodes emitting around 830 nm for optical stimulation, and a U340 detection filter pack to detect in the region 270-380 nm (Bøtter-Jensen et al., 1997; 2000).

Equivalent dose determinations were performed on sets of 16 aliquots per sample, using a SAR sequence (Murray and Wintle, 2000). Using this procedure, the OSL signal levels from each individual disc were calibrated to provide an absorbed dose estimate (the equivalent dose) using an interpolated dose-response curve, constructed by regenerating OSL signals by beta irradiation in the laboratory. Sensitivity changes which may occur as a result of readout, irradiation and preheating (to remove unstable radiation-induced signals) were monitored using small test doses after each regenerative dose. Each measurement was standardized to the test dose response determined immediately after its readout, to compensate for changes in sensitivity during the



laboratory measurement sequence. The regenerative doses were chosen to encompass the likely value of the equivalent (natural) dose. A repeat dose point was included to check the ability of the SAR procedure to correct for laboratory-induced sensitivity changes (the ‘recycling test’), a zero dose point is included late in the sequence to check for thermally induced charge transfer during the irradiation and preheating cycle (the ‘zero cycle’), and an IR response check included to assess the magnitude of non-quartz signals. Regenerative dose response curves were constructed using doses of 2.5, 5.0, 10, 20 and 30 Gy, with test doses of 1.0 Gy. The 16 aliquot sets were sub-divided into four subsets of four aliquots, such that four preheating regimes were explored (200°C, 220°C, 240°C and 260°C).

## 4. Results and discussion

### 4.1. OSL ages at the three transects

OSL dating results are presented in Table 1 and Figs. 4, 5 and 6. At Santa Cruz Transect we observed that ages progressively increase from the shoreline to farther inland among Nay1 and Nay7 (see Figs. 4 and 7). Sample Nay8, that is the most inland sample, breaks this age increasing progression as Nay7 is  $2.097 \pm 0.14$  ka and Nay8 is  $1.611 \pm 0.099$  ka. We think that a plausible reason for Nay8 being younger than expected in this succession is related to its proximity to the lagoon area of the coastal plain. As this area is 1-2 meters lower in elevation than the beach-dune ridges, it is prone to flooding during eventual high-discharges of rivers (Ortiz-Pérez, 1979). During these flooding events, recent sediment is delivered, and we propose that some of these recent sediments arriving to the lagoon’s area partially covers the sediment of old beach-dune ridges as these are more compacted than the sediment located towards the shoreline. As a consequence, it is highly possible that some recent sediment could settle around the site where Nay8 was extracted and in this resulting in an inversion of age progression at Nay8. This same inversion on age progression was observed at Novillero Transect. Here, our results indicated that sample Nay10 ( $2.431 \pm 0.187$  ka) is older than Nay9 ( $0.139 \pm 0.038$  ka), as it was expected but, sample Nay11 ( $1.178 \pm 0.116$  ka) is younger than sample Nay10. In this case, the sample Nay11 was extracted just behind the lagoon’s area (see Fig. 5).

At Toro Mocho Transect we found a good progression of ages from the shoreline to inland; except for samples Nay12 ( $0.476 \pm 0.057$  ka) and Nay13 ( $0.418 \pm 0.048$  ka). However, as sites Nay12 and Nay13 are less than 1 km of distance and the difference in age is only of 58 years, the distance-age inversion found could be a result of the uncertainty obtained for both samples. Thus, we considered that both Nay12 and Nay13 are still confirming the progression sequence of OSL ages along the Toro Mocho transect (Fig. 7).

### 4.2. Landscape evolution of the strand-plain of Nayarit

The oldest luminescence results in the three transects are located in the beach-dune ridges situated in the most inland sectors of the strand-plain of Nayarit. These values are of  $2.097 \pm 0.14$  ka (Nay7) in the transect of Santa Cruz,  $2.431 \pm 0.187$  ka (Nay10) in the transect of Novillero and  $1.763 \pm 0.115$  ka (Nay16) in the transect of Toro Mocho. These OSL results are consistently providing an age of about 2 ka (as the mean value is  $2.1 \pm 0.35$  ka) for the oldest beach-dune ridges and therefore, they indicate that the strand-plain should have initiated about



this age from north to south. These OSL ages yield new data about the age of the strand-plain since it is younger than it was thought previously by Curray et al. (1969) and Abe Cisneros (2011), whose estimated an initiation age of 5.7 - 4.5 ka. These studies were based their interpretation on radiocarbon dating. We recalculated the different periods of shoreface succession based on our OSL results, which are presented in Table 2, where we also included the periods presented by Curray et al. (1969) and Abe Cisneros (2011) for comparison.

We plotted the resulting ages and the distance from the samples' location to their closest shoreline positions; which were traced as perpendicular straight lines to most of the beach-dune ridges. We obtained a tight correlation of  $R^2 = 0.95$  when plotting distance and OSL ages for the case of the transects of Santa Cruz and Toro Mocho (Fig. 7) what suggest a constant rate of aggradation of beach-dune ridges in the central and southern sectors of the strand-plain.

We calculated the beach-dune ridges depositional rates at the sectors of the strand-plain where we extracted samples. To do that, we used the oldest OSL ages of each transect and the distance from the samples' location to their closest shoreline position; which were traced as a straight line perpendicular to most of the beach-dune ridges. For the Santa Cruz Transect we obtained a depositional rate of  $5.98 \text{ m a}^{-1}$  between the shoreline and Nay7 (that is 12.55 km far from the coastal line). For Novillero Transect we calculated  $1.76 \text{ m a}^{-1}$  between the shoreline and sampling site Nay10 (that is 4.07 km to the coastal line) and for Toro Mocho  $5.18 \text{ m a}^{-1}$  between the shoreline and sampling site Nay16 (that is 9.13 km to the coastal line). The highest depositional rate corresponds to Santa Cruz Transect, which is the widest sector of the strand-plain of Nayarit, such rate is similar as the one we estimated for Toro Mocho Transect. Therefore, the depositional rate at the strand-plain drops towards the north where it is located the transect of Novillero. The highest depositional rates of Santa Cruz and Toro Mocho transects are due to stream discharge because the source of sediment from the highlands to the coastal plain and to the sea (and in this case, back to the strand-plain) mainly comes from the Santiago and San Pedro rivers, as Abe Cisneros (2011) previously identified.

The depositional rates between  $6$  and  $1.8 \text{ m a}^{-1}$  in the strand-plain of Nayarit are indicating that progradation rate is slightly lower than those reported for the strand-plain of the Usumacinta and Grijalva rivers that are estimated in  $4.7$  to  $8.8 \text{ m a}^{-1}$  (Muñoz-Salinas et al., 2017). The depositional rates of the Nayarit strand-plains are, however, high in comparison to those rates reported in other strand-plains around the world. For instance, the depositional rate found for Phra Thong Island in Thailand is  $2.7 \text{ m a}^{-1}$  (Brill et al., 2012), in Merrit Island, Florida is  $1.57 \text{ m a}^{-1}$  (Rink and Forrest, 2005), for the Apalachicola Barrier, also in Florida, is  $0.08 \text{ m a}^{-1}$  (Rink and López, 2010), in SW Australia the rate has been estimated in  $0.57 \text{ m a}^{-1}$  (Thom et al., 1978), Guichen Bay, southern Australia is  $0.38 \text{ m a}^{-1}$  (Murray-Wallace et al., 2002). We only found that the reported depositional rate for the strand-plain of Skalligen Spit in Denmark of  $30 \text{ m a}^{-1}$  (Aagaard et al., 2007) and the Usumacinta and Grijalva strand-plain being are higher than the rate estimated for the case of Nayarit.

Finally, we propose here a simplified age model for the initiation of the coastal plain of Nayarit by assuming two conditions: (1) a constant depositional rate of  $5.98 \text{ m a}^{-1}$  that is the depositional rate obtained at Santa Cruz Transect and (2) a lack of erosion on the sediment deposited in the coastal plain since the moment it emerged. Then, as the coastal plain (lowlands)

extends from the current shoreline to the contact with the highlands a distance of 37-42 km (see the coastal plain limit in Fig. 1), we calculated that the coastal plain of Nayarit initiated 6-7 ka. This moment of initiation is consistent with the time when sea-level rise started to cease in the Gulf of Mexico, which is at about 7 ka (Balsillie and Donoghue, 2004; Davis, 2011).

## 5. Conclusions

We present here the first complete geochronological record of the strand-plain of Nayarit. This is based on the luminescence dating of 16 sediment samples extracted from beach-dune ridges located along three different transects (from W-E) that almost perpendicularly cut the ridges oriented from N-S and from NNW to SSE along the coast. OSL measurements were conducted on quartz grains following a SAR protocol and combined with dose rate measurements (HRGS and TSBC) on these samples. The resulting OSL ages show a similar pattern, in which ages increase from the shoreline to farther inland.

The oldest luminescence ages in the three transects are consistently indicating that the strand-plain initiated approximately 2 ka. Depositional ages calculated from luminescence results provide progradational rates between 6.0 to 1.8 m a<sup>-1</sup>, the highest one is towards the southern part of the strand-plain where the largest rivers flow into the area (which are the rivers Santiago and San Pedro) and the lowest rates located towards the northern part where the smallest rivers flow into.

Using the largest depositional rates estimated from the OSL results and distance of the sampling sites to the current shoreline we calculated that the coastal plain of Nayarit should have initiated about 6-7 ka; which is the time when sea level raise stabilized worldwide.

## Acknowledgements

This work was supported by grant UNAM-DGAPA-PAPIIT number IN105517. Authors thank the following students for their help during field work: Andrés Lallande, Salvador Ponce, Jorge Zavala and Arturo Godinez. Authors also thank to Dr. Hernández Santana and an anonymous review for their thoughtful comments which helped to improve the final version of this paper.

## References

- Aitken, M. J. 1998. *An Introduction to Optical Dating. The Dating of Quaternary Sediments by the Use of Photon Stimulated Luminescence*. New York: Oxford University Press.
- Aagaard, T.J., Orford, J., Murray, A.S., 2007. Environmental controls on coastal dune formation: Skallingen Spit, Denmark. *Geomorphology* 83, 29-47.
- Abe Cisneros, R., 2011. Provenance and Origin of Holocene Beach Ridge and Modern Beach Sands from the Costa de Nayarit, Western Mexico. Ms Thesis submitted to Louisiana State University and Agricultural and Mechanical College, USA.

Balsillie, J.H., Donoghue, J.F., 2004- High Resolution Sea-level History for the Gulf of Mexico since the Last Glacial Maximum. Florida Geological Survey Report of Investigations. Tallahassee: Florida.

Bøtter-Jensen L. 1997. Luminescence techniques: instrumentation and methods. *Radiation Measurements* 27: 749–768.

Bøtter-Jensen L. 2000. Development of Optically Stimulated Luminescence Techniques using Natural Minerals and Ceramics, and their Application to Restrospective Dosimetry. Risø-R-1211(EN), Dsc. Thesis. Risø National Laboratory.

Brill, D., Klasen, N., Brueckner, H., Jankaew, K., Scheffers, A., Kelletat, D., Scheffers, S., 2012. OSL dating of tsunami deposits from Phra Thong Island, Thailand. *Quaternary Geochronology* 10, 224-229.

Brill D, Jankaew K and Brückner H, 2015. Holocene evolution of Phra Thong's beach-ridge plain (Thailand)—Chronology, processes and driving factors. *Geomorphology* 245: 117–134, DOI 10.1016/j.geomorph.2015.05.035.

Cresswell, A., Sanderson, D., Muñoz-Salinas, E., Castillo, M., 2017. Luminescence dating of Beach Dunes and Fluvial Sediments. OSL Dating Report. SUERC.

Cruz González, M., 2012. Variaciones estacionales en la línea de costa entre el canal de Cuautla y el estero de San Cristobal, Nayarit. Bachelor Thesis, Facultad de Filosofía y Letras, UNAM, Mexico.

Curray, J.R., Moore, D.G., 1964. Holocene regressive littoral sand, costa de Nayarit, Mexico. In: *Deltaic and Shallow Marine Deposits* (Ed:van Straaten, L.M.J.U.). Elsevier Publishing Company, Amsterdam.

Curray, J.R., Emmel, F.J., Crampton, P.J.S., 1969. Holocene history of a strand plain, lagoonal coast, Mexico, in *Lagunas Costeras, Un Simposio, UNAM-UNSECO, Nov. 28-30, 1967 en Mexico*, pg. 63-100

Davis, R.A., 2011. *Sea-level Change in the Gulf of Mexico*. Texas A&M University Press.

Duller, G.A., 2008. Single-grain optical dating of Quaternary sediments: why aliquot size matters in luminescence dating. *Boreas* 37: 589-612

Hudson, P., Hendrickson, D.A., Benke, A.C., Varela-Romero, A., Rodiles-Herández, R. and Minckley, W.L., 2005. Rivers of Mexico. In: Benke, A.C. and Cushing, C.E. (eds), *Rivers of North America*. Elsevier Academic Press, San Diego, CA.

Huntley DJ, Godfrey-Smith DI, Thewalt MLW. 1985. Optical dating of sediments. *Nature* 313: 105–107.

- Isla FI and Bujalesky GG, 2000. Cannibalisation of Holocene gravel beach-ridge plains, northern Tierra del Fuego, Argentina. *Marine Geology* 170: 105–122, DOI 10.1016/S0025-3227(00)00069-4.
- Murray-Wallace, C.V., Banerjee, D., Bourman, R.P., Olley, J.M., Brooke, B.P., 2002. Optically stimulated luminescence dating of Holocene relict foredunes, Guichen Bay, South Australia. *Quat. Sci. Rev.* 21, 1077-1086.
- Muñoz-Salinas, E., Castillo, M., 2013. Sediment and water discharge assessment on Santiago and Pánuco rivers (Central Mexico): The importance of topographic and climatic factors. *Geografiska Annals series A, Physical Geography* 95: 171-183.
- Muñoz-Salinas, E., Castillo, M., Sanderson, D., Kinnaird, T., 2017. Geochronology and landscape evolution of the strand-plain of the Usumacinta and Grijalva rivers, southern Mexico. *Journal of South American Earth Sciences* 79, 394-400.
- Nordstrom, K., Psuty, N., Carter, B., 1991. *Coastal Dunes: Form and Process*. John Wiley and sons.
- Ortiz-Pérez, M.A., 1979. Fotointerpretación geomorfológica del curso bajo del río Grande de Santiago, Nayarit. *Invest. Geog.* 9: 65-92.
- Otvos, E.G., 2000. Beach ridges – definitions and significance. *Geomorphology* 32, 83-108.
- Prescott, JR, Hutton, JT. 1994. Cosmic ray contributions to dose rates for luminescence and ESR dating: large depths and long-term time variations. *Radiation Measurements* 23: 497–500
- Nordstrom, K., Psuty, N., Carter, B. 1990. *Coastal Dunes Form and Process*. John Wiley & Sons, Chichester.
- Nielsen A, Murray AS, Pejrup M and Elberling B, 2006. Optically stimulated luminescence dating of a Holocene beach ridge plain in Northern Jutland, Denmark. *Quaternary Geochronology* 1: 305– 312, DOI 10.1016/j.quageo.2006.03.001.
- Reimann T, Tsukamoto S, Harff J, Osadczuk K and Frechen M, 2011a. Reconstruction of Holocene coastal foredune progradation using luminescence dating—An example from the Świna barrier (south- ern Baltic Sea, NW Poland). *Geomorphology* 132: 1–16, DOI 10.1016/j.geomorph.2011.04.017.
- Rink, W.J., Forrest, B., 2005. Dating evidence for the accretion history of beach ridges on Cape Canaveral and Merrit Island, Florida, USA. *J. Coast. Res.* 21, 1000-1009.
- Rink, W.J., López, G.I., 2010. OSL-based lateral progradation and Aeolian sediment accumulation rates for the Apalachicola Barrier Island Complex, North Gulf of Mexico, Florida. *Geomorphology* 123, 330-342.

- Sanderson, D.C.W., 1988. Thick source beta counting (TSBC): A rapid method for measuring beta dose-rates: *International Journal of Radiation Applications and Instrumentation. Part D. Nuclear Tracks and Radiation Measurements* 14: 203-207.
- Tamura, T., 2012. Beach ridges and prograded beach deposits as palaeoenvironment records. *Earth-Science Reviews*, 2121, **114**, 279-297.
- Tamura, T., Ito, K., Inoue, T., Sakai, T., 2017. Luminescence Dating of Holocene beach-dune ridge sands on the Yumigahama Peninsula, western Japan. *Geochronometria* 44: 331-340.
- Thom, B.G., Polach, H.A., Bowman, G.M., 1978. Holocene Age Structure of Coastal Sand Barriers in New South Wales, Australia. Geography Department Report. Duntroon: University of New South Wales.
- Wintle AG, Murray AS. 2006. A review of quartz optically stimulated luminescence characteristics and their relevance in single-aliquot regeneration dating protocols. *Radiation Measurements* 41: 369–391.

## Figure captions

**Figure 1.** Location of the beach-dune ridges composing the strand-plain of Nayarit in west-central Mexico. The main rivers draining to the coast of Nayarit are delineated, the largest one is Santiago River Basin which denudates part of the Trans-Mexican Volcanic Belt and the Sierra Madre Occidental. Santiago River is the largest river in the area, followed by San Pedro, Acaponeta and Las Cañas, these three are sourced in the Sierra Madre Occidental. Red line indicates the limit of the map presented in Fig. 2. The base map was obtained from the SRTM digital elevation data of 90 m produced by NASA and downloaded from: <http://www.cgiar-csi.org>

**Figure 2.** Location of OSL sites in the strand-plain of Nayarit. OSL sites are arranged in three transects that from north to south are called as: Novillero, Santa Cruz and Toro Mocho. Red lines indicate main changing directions of beach-dune ridges and roman numbers the five different periods of shoreface succession based on interpretations of Curray et al. (1969). Based map is a satellite image Landsat 8 from NASA downloaded from: <https://landsat.usgs.gov>

**Figure 3.** Pictures of beach-dune ridges of the strand-plain of Nayarit. We observed well-preserved beach-dune ridges and mangrove across the transect of Santa Cruz in (A) and (B). In this transect it is easy to recognize the crests and swales of beach-dune ridges as swales are usually with water. We found that across the transects of Novillero (C) and Toro Mocho (D) human activities based on agriculture have almost totally destroyed the mangrove. Beach-dune ridges in these two transects are difficult to recognized as the first centimeters of soil have been plowed. OSL samples extracted across Novillero and Toro Mocho transects were extracted at deeper depths of 80 cm to avoid the effect of plowed soils.

**Figure 4.** Site location of samples Nay1 to Nay8 across the transect of Santa Cruz. We observe a progressive increase of ages from the samples close to the shoreline to those located farther inland except for sample Nay8 which is the closest sample to the lagoon area which is prone to flooding and therefore, to receive young sediment. We have marked the five different periods of shoreface succession based on interpretations of Curray et al. (1969).

**Figure 5.** Site location of samples Nay9 to Nay11 across the transect of Novillero. We observe a progressive increase of ages from Nay9 to Nay10 but sample Nay11 is providing a younger age than expected, however we observed (as for Nay8) that this sample is very close to the lagoon area which is prone to flooding.

**Figure 6.** Site location of samples Nay12 to Nay16 across the transect of Toro Mocho. We observe a progressive increase of ages from the samples close to the shoreline to those located farther inland except for samples Nay12 and Nay13. See in the text a plausible explanation for this age inversion.

**Figure 7.** Plot of age versus distance from the shoreline for samples located across the transect of Santa Cruz (yellow dots) and Toro Mocho (red dots); except for sample Nay8 as this age is



highly possible rejuvenated by younger sediment coming from the lagoon area (see discussion in the text). We observe a very good correlation of ages versus distance with support a progressive depositional rate of sediment in the strand-plain of Nayarit.

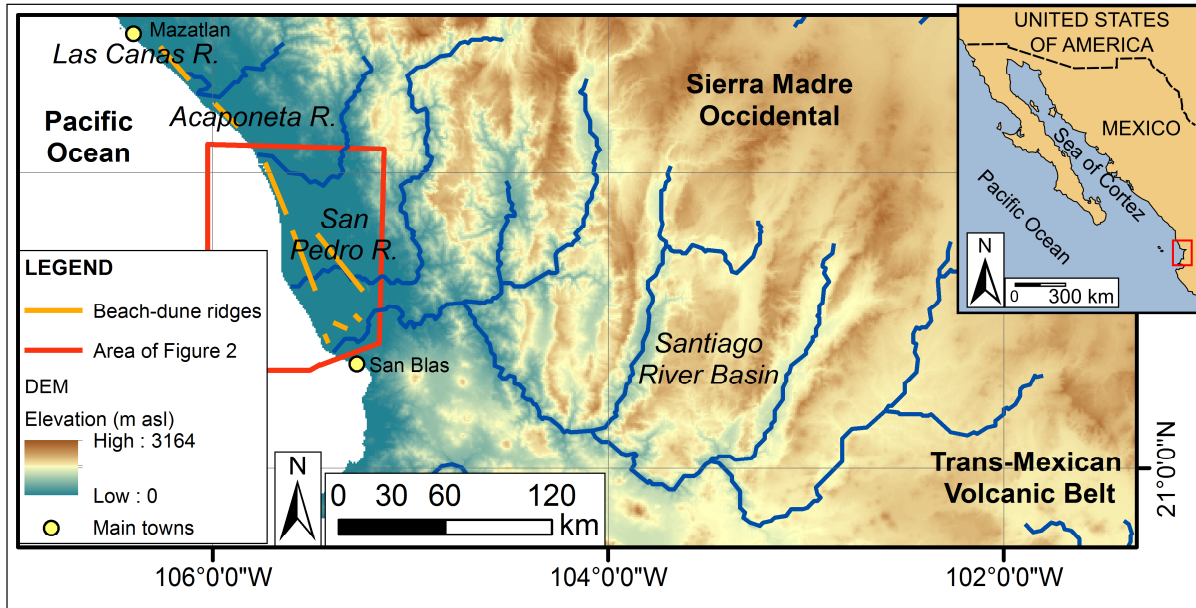
ACCEPTED MANUSCRIPT

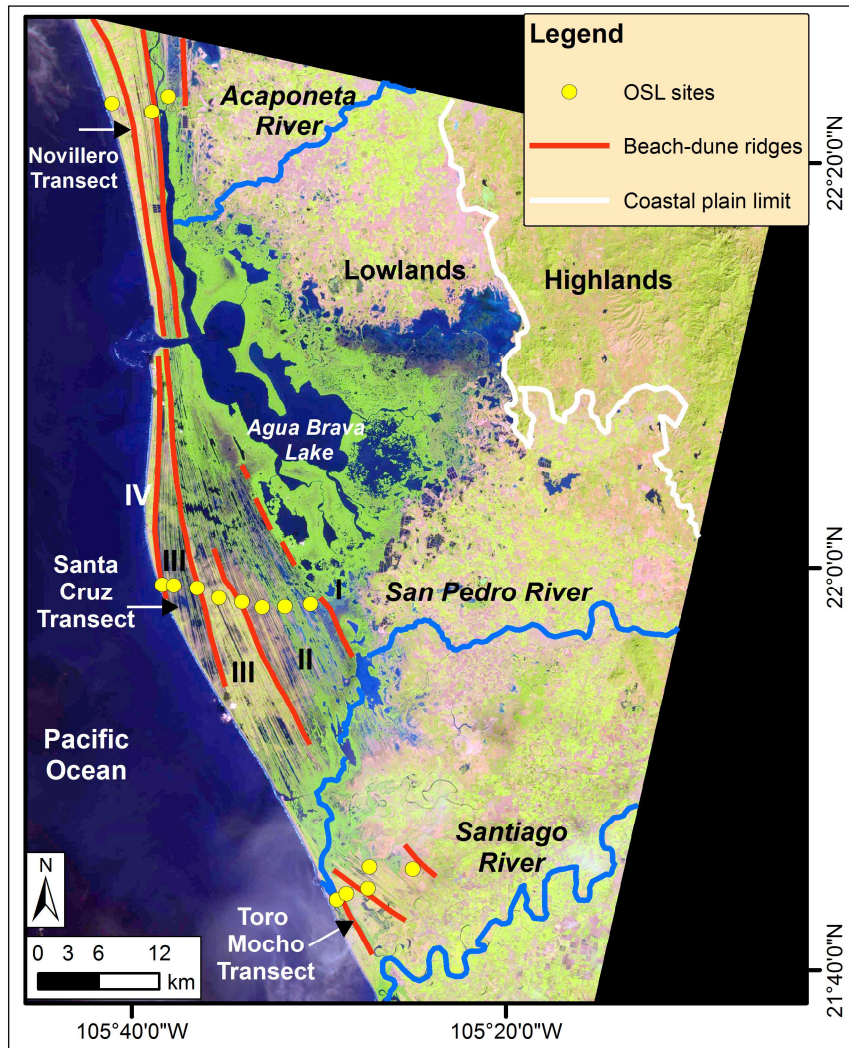
**Table 1.** Sample names, location and OSL results obtained for the sixteen sites around the strand-plain of Nayarit (For further details on the analytical procedures consult the laboratory report of Cresswell et al., 2017).

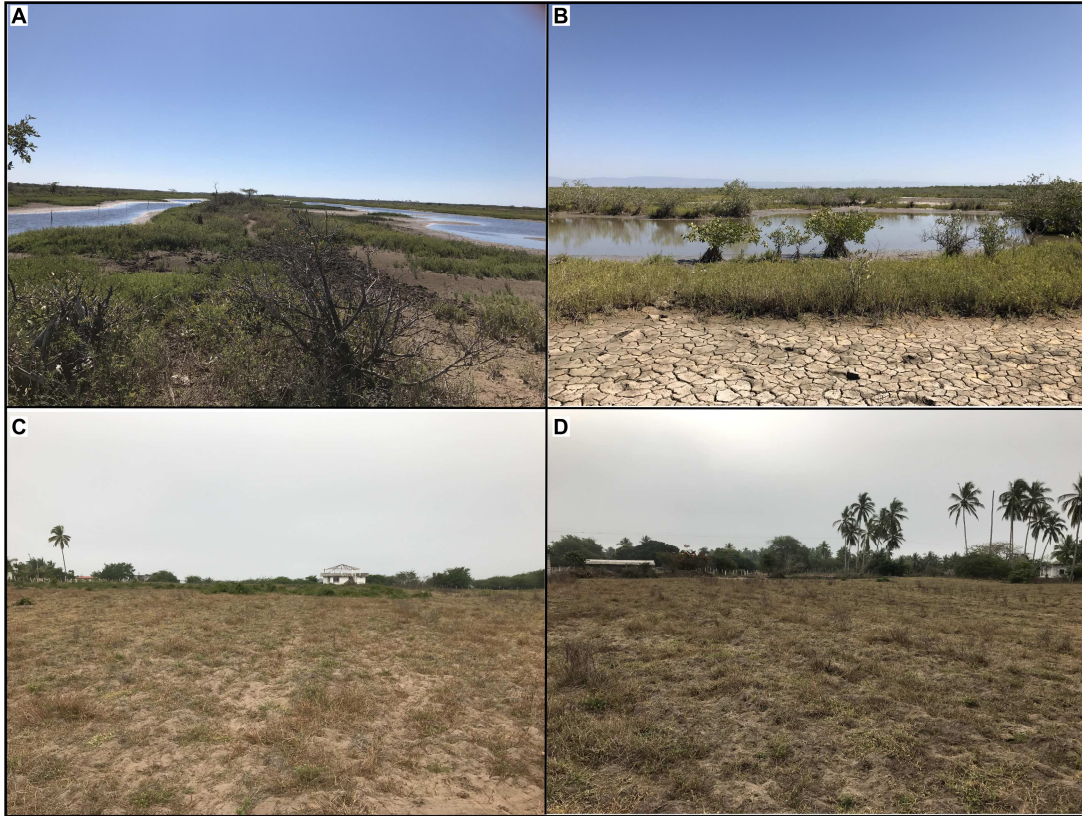
Code	Lab code/SUTL no.	Northing	Easting	Transect	Equivalent Dose (Gy)	Dose Rate (mGy a <sup>-1</sup> )	Years / ka	Calendar years
Nay1	2941	433974	2431427	Santa Cruz	1.29 ± 0.08	3.01 ± 0.14	0.429 ± 0.033	1588 ± 33 AD
Nay2	2942	435040	2431367		1.95 ± 0.17	3.35 ± 0.15	0.582 ± 0.057	1435 ± 57 AD
Nay3	2943	437186	2431112		2.51 ± 0.22	2.97 ± 0.13	0.845 ± 0.083	1172 ± 83 AD
Nay4	2944	439182	2430213		2.77 ± 0.32	3.10 ± 0.14	0.894 ± 0.111	1123 ± 111 AD
Nay5	2945	441320	2429803		3.39 ± 0.27	2.24 ± 0.09	1.513 ± 0.135	504 ± 135 AD
Nay6	2946	443175	2429298		6.32 ± 0.53	3.30 ± 0.15	1.915 ± 0.183	102 ± 183 AD
Nay7	2947	445251	2429370		6.08 ± 0.32	2.90 ± 0.12	2.097 ± 0.14	80 ± 140 BC
Nay8	2948	447623	2429581		5.06 ± 0.15	3.14 ± 0.17	1.611 ± 0.099	406 ± 99 AD
Nay9	2949	429559	2475342	Novillero	0.49 ± 0.13	3.52 ± 0.18	0.139 ± 0.038	1878 ± 38 AD
Nay10	2950	433224	2474587		6.83 ± 0.38	2.81 ± 0.15	2.431 ± 0.187	414 ± 187 BC
Nay11	2951	434745	2475987		4.03 ± 0.36	3.42 ± 0.14	1.178 ± 0.116	839 ± 116 AD
Nay12	2952	449934	2402510	Toro Mocho	1.27 ± 0.14	2.67 ± 0.12	0.476 ± 0.057	1541 ± 57 AD
Nay13	2953	450842	2403067		1.45 ± 0.15	3.47 ± 0.17	0.418 ± 0.048	1599 ± 48 AD
Nay14	2954	452801	2403529		3.16 ± 0.17	3.67 ± 0.17	0.861 ± 0.061	1156 ± 61 AD
Nay15	2955	452956	2405483		2.73 ± 0.21	2.85 ± 0.13	0.958 ± 0.086	1059 ± 86 AD
Nay16	2956	456934	2405273		5.59 ± 0.27	3.17 ± 0.14	1.763 ± 0.115	254 ± 115 AD

**Table 2.** Comparison of the periods forshoreface construction at the strand-plain of Nayarit between the data provided by Curray et al. (1969) and Abe Cisneros (2011) based on radiocarbon dating and the results of this paper at Santa Cruz Transept based on luminescence dating.

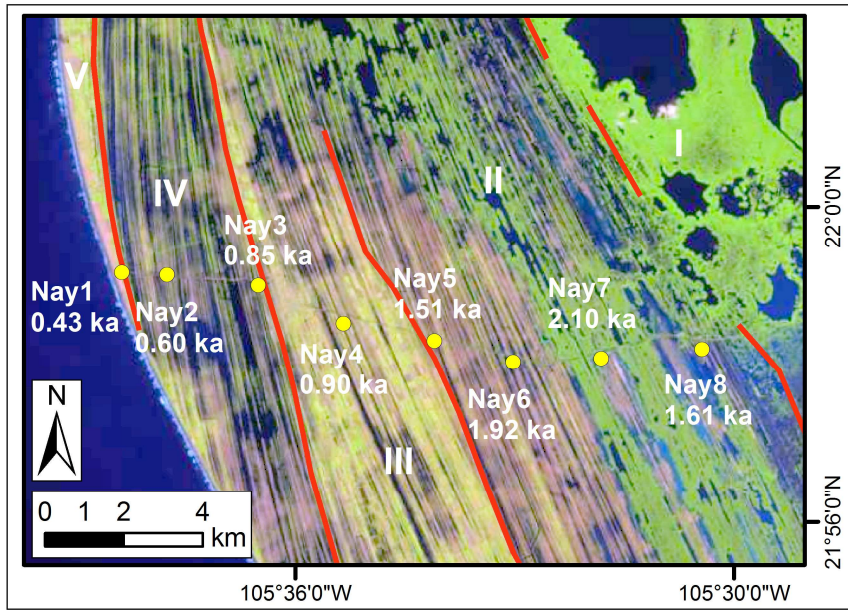
<b>Periods of shoreface succession</b>	<b>Curray et al. (1969) and Abe Cisneros (2011)</b>	<b>This paper at Santa Cruz Transept</b>
I	4.7 - 4.5 ka	> 2 ka
II	4.5 - 3.6 ka	2 - 1.5 ka
III	3.6 - 1.5 ka	1.5 - 0.8 ka
IV	1.5 - 0.5 ka	0.8 - 0.4 ka
V	< 0.5 ka	< 0.4 ka

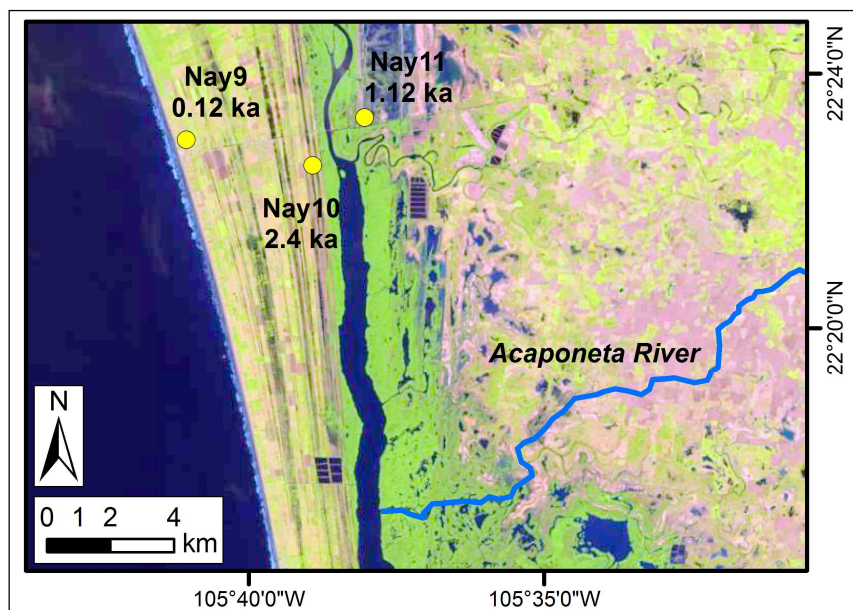


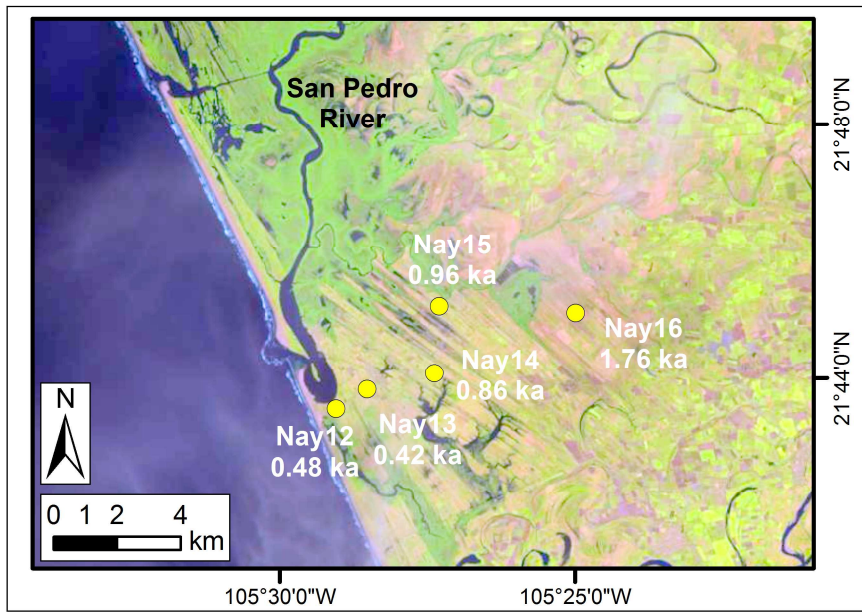


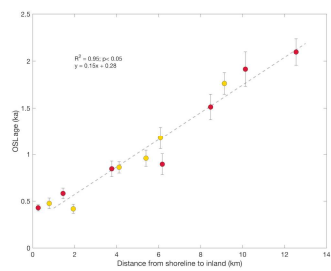












ACCEPTED MANUSCRIPT

- A robust OSL geochronological record for the strand-plain of Nayarit
- The strand-plain of Nayarit initiated about 2 ka
- Aggradation of the coastal plain of Nayarit initiated about 6-7 ka

ACCEPTED MANUSCRIPT